

1986

Dimensional Optimization of Scroll Compressors

J. W. Bush

J. Caillat

S. M. Seibel

Follow this and additional works at: <https://docs.lib.purdue.edu/icec>

Bush, J. W.; Caillat, J.; and Seibel, S. M., "Dimensional Optimization of Scroll Compressors" (1986). *International Compressor Engineering Conference*. Paper 574.
<https://docs.lib.purdue.edu/icec/574>

This document has been made available through Purdue e-Pubs, a service of the Purdue University Libraries. Please contact epubs@purdue.edu for additional information.

Complete proceedings may be acquired in print and on CD-ROM directly from the Ray W. Herrick Laboratories at <https://engineering.purdue.edu/Herrick/Events/orderlit.html>

DIMENSIONAL OPTIMIZATION OF SCROLL COMPRESSORS

James W. Bush Jean-Luc Caillat Stephen M. Seibel
Sr. Proj. Eng. Proj. Manager Proj. Engineer

Research and Development Department
Copeland Corporation
Sidney, Ohio, U.S.A.

ABSTRACT

An analytical model is developed, which includes mechanical, electrical, and compression power losses, volumetric efficiency, heat transfer, and oil circulation. Each loss component is expressed in terms of empirically determined constants and fundamental dimensional parameters. The dimensions optimization is carried out utilizing a computerized model which varies the fundamental parameters within design constraints.

INTRODUCTION

Mathematical modeling of well known positive displacement compressors has been increasingly refined and well publicized in the last fifteen years. Models widely varying in scope as well as complexity have been developed and have significantly contributed to the advancement of the latest generation of compressors. In contrast, however, only a few studies devoted to the more recently investigated scroll compressor have been published.

The study presented in the following paper, while including a few similarities in its conceptual approach, departs from earlier works in that it addresses the general scroll compressor design methodology. The two major objectives of the analysis are (1) to determine the dimensional optimization, (2) to predict the performance potential for various displacement scroll compressors.

The analytical model resulted in optimization of the basic dimensional parameters of the scroll

compressor to maximize the efficiency. The various loss terms associated with individual models representing functional elements were dimensionally scaled, semi-empirically evaluated using coefficients determined from experimental results, and finally combined into the efficiency equation based on a First Law energy model of the overall compressor. The model was computerized as an accumulation of individual models to facilitate refinements or additions.

BACKGROUND

Although the scroll mechanism was described by Léon Creux in 1905 [1] and subsequent variations or improvements were shown shortly thereafter [2][3], little activity towards its commercialization as a compressor was generated until the 1970s. The primary reasons for such renewed interest in the scroll mechanism as a compressor are: (1) cost effectiveness as a result of major improvements in manufacturing techniques, (2) high performance potential in terms of efficiency, noise, and pulsation at conventional and higher speeds.

Scroll Members

Conventional scroll members are mirror-imaged pairs comprising a single appropriately shaped spiral vane, of uniform thickness and height, protruding from an end plate. Spirals of the involute type are most commonly used, particularly the involute of a circle.

This type of scroll was investigated throughout the present paper. The basic parameters defining the scrolls are displayed on Fig. (1). They are generating radius, R_g ; orbiting radius, R_{or} ; vane height, H ; vane thickness, T .

It is worth mentioning that functional scrolls, in which vanes are dissimilar in shape or of non-uniform thickness or height have been devised.

Principle of Operation

The members are appropriately phased, and eccentrically mated, so as to form various pockets bounded by the vanes and their respective end plates, as shown in Fig. (2). Most commonly, one scroll is fixed and the other made to orbit by a crank mechanism. Through relative motion of the members the pockets, initially opened to the surroundings, are first formed, sealed off, progressively moved inwards while reducing in volume, and finally merged into a common discharge volume. (See Fig. (2) - a, b, c, d).

Conversely, simultaneous rotation of the members about their respective geometric center yields an equivalent relative motion of the members. However, the first scheme only was considered in the present paper.

The inherent advantages of such a scroll mechanism are valveless compression, virtually constant volumetric efficiency, nearly continuous suction and discharge flow, smooth operation, low relative velocity and potentially low unbalance.

Integral Compressor Design

A conceptualized schematic, showing the various functional elements of the scroll compressor used in the present analysis, is displayed in Fig. (3). This is the "basic" compressor from which the First Law model was derived.

FIRST LAW MODEL

A schematic of the compressor model is shown in Figure (4). The compressor shell forms a control volume through which refrigerant vapor flows, electrical energy is input, and some heat is transferred. Within the shell control volume are four secondary control volumes:

- (1) Vapor in the shell, through which the suction gas flows and to and from which waste heat is transferred.
- (2) The electric motor which converts electrical energy into mechanical energy and some waste heat.
- (3) The compressor running gear (bearings, etc.) which transfer the mechanical energy to the compression process while converting some of it to waste heat.
- (4) The scroll set in which the compression process takes place. The refrigerant flows through the set (and on out of the shell control volume). Mechanical energy is input from the running gear and some waste heat is generated.

First Law equations for each of these control volumes are used to expand the efficiency equation.

General Assumptions

Before expanding the efficiency equation, some assumptions were made:

- (1) It was assumed that all compressors would be driven by 60 Hz, 2-pole induction motors at a constant speed of roughly 3450 rpm.
- (2) The compressor is used for air conditioning and heat pump applications. The rating condition chosen for the study is the American Refrigeration Institute air conditioning rating point (ARI A/C) using Freon-22 as a refrigerant. The conditions are 130°F condensing temperature, 15°F liquid subcooling, 45°F evaporating temperature, and 20°F vapor superheating.
- (3) Since the scroll compressor is a fixed volume ratio device, a single volume ratio R_v was chosen for the study. The chosen ratio was not necessarily the optimum for the chosen operating condition.
- (4) Given a constant volume ratio and assuming equal wrap angles, the proportionality relation governing displaced volume is

$$V_c \propto R_g R_{or} H$$

- (5) A constant percentage by weight of oil circulating with the refrigerant in the system was chosen independently of compressor capacity since it is controllable through design.
- (6) Finally, ideal gas behavior of the refrigerant vapor with a polytropic coefficient of 1.18 was assumed for the compression process.

Efficiency Definition

Compressor efficiency is usually defined as some modified form of the coefficient of performance at a specified condition of evaporating and condensing temperatures and of refrigerant superheating and subcooling.

$$\text{Efficiency, } \eta = \frac{\text{Evaporator heat, } Q_e}{\text{Input Power, } W_{in}}$$

If the operating condition is known, the capacity may be expressed as a function of refrigerant mass flow rate.

$$\eta = \frac{Q_e (\dot{m}_r)}{W_{in}}$$

This equation for efficiency forms the basis of the compressor model.

Capacity Term

At the ARI A/C condition, the capacity term in the efficiency equation becomes

$$Q_e = \Delta h_e \dot{m}_r - \Delta h_o \dot{m}_o$$

The refrigerant mass flow may be further expressed as

$$\dot{m}_r = \dot{V}c \eta_v (\rho_{65} \eta_{ph})$$

The preheat efficiency represents the expansion of refrigerant vapor in the shell prior to suction at the scrolls. It may be represented by a specific volume ratio and was approximated using a linear curve fit of the refrigerant enthalpy chart.

$$\eta_{ph} = \frac{H_{65}}{Ca + Cb Ts} = \frac{H_{65}}{H_{65} + \Delta H}$$

This may be checked iteratively by comparing the result to the calculated enthalpy increase. The enthalpy increase is the sum of the waste heat and shell heat loss.

$$\Delta H = Q_w + Q_s$$

The oil circulation rate is given by

$$\dot{m}_o = Ro \dot{m}_r$$

Using the two mass flow relations, the capacity term becomes

$$Q_e = (\Delta h_e - \Delta h_o Ro) (\dot{V}c \eta_v \rho_{65} \frac{H_{65}}{H_{65} + \Delta H})$$

and needs not to be expanded further until individual scaling relations are considered.

Power Term

The power term in the efficiency equation may be written as

$$W_{in} = (W_p + L_c + L_m) \frac{1}{\eta_m}$$

The polytropic compression power is simply

$$W_p = \frac{n}{n-1} (P_d/R_v - P_s) \dot{V}_c$$

The mechanical loss may be partitioned into

$$L_m = L_j + L_t + L_f$$

With further expansion limited to the scaling relations, the power term was

$$W_{in} = \left[\frac{n}{n-1} (P_d/R_v - P_s) \dot{V}_c + L_c + L_j + L_t + L_f \right] \frac{1}{\eta_m}$$

CAPACITY SCALING RELATIONS

It was stated earlier that the compressor displacement is proportional to R_g , R_{or} , and H . These three were the independent variables for which the optimization was performed. The first scaling relation was

$$V_c = C_o R_g R_{or} H$$

Since the design to be analyzed was radially compliant with a given fixed tip clearance (no tip seals were used), flank leakage was assumed to be (nearly) zero and the tip clearance was scaled proportionately to the flank height plus some minimum clearance. The smallest minimum clearance is limited only by the actual part and assembly tolerances.

$$\delta = \delta_m + C_1 H$$

Because pressure drops in the shell were neglected, a constant pressure enthalpy rise during the preheat process was assumed. Also assumed was that any oil circulating in the system stays with the suction vapor during preheat and enters the scroll set at the same temperature.

Volumetric Efficiency

Calculation of volumetric efficiency was based on a tip leakage calculation between the first sealed pocket and suction conditions for a complete shaft revolution. The flow was treated as Fanno flow, i.e.

adiabatic through a narrow channel with friction [4]. The length of the channel (vane thickness) was

$$T = \pi R_g - R_{or}$$

The channel width and height were proportional to R_g and R_{or} respectively.

Beginning with the preceding assumptions and conditions, the expression used for volumetric efficiency was

$$\eta_v = 1 - C_2 \frac{(\delta + \delta_{\min})^{C_{12}}}{R_{or} H \sqrt{\pi R_g - R_{or} + C_3 (\delta + \delta_{\min})}}$$

The "minimum" tip clearance, δ_{\min} , was determined by the potential composite runout of the mating surfaces of the scroll set.

Preheat Efficiency

The waste heat Q_w may be broken down into

$$Q_w = W_{in}(1 - \eta_m) + L_j + L_t + L_f + Q_c$$

and the capacity equation becomes

$$Q_e = (\Delta h_e - \Delta h_o R_o) (\dot{V}_c \eta_v \rho_{65})$$

$$\frac{H_{65}}{H_{65} + W_{in}(1 - \eta_m) + L_j + L_t + L_f + Q_c}$$

The motor and mechanical loss terms will be discussed shortly.

The compressor and shell heat loss term was assumed to be proportional to a scroll surface area approximation,

$$Q_c = C_4 (R_g R_{or} H)^{2/3}$$

$$Q_s = C_5 (R_g R_{or} H)^{2/3}$$

Which assumes similar compressor-vapor temperature differences. The compressor heat loss Q_c includes waste heat from the discharge plenum and tube.

POWER SCALING RELATIONS

The polytropic power expression was introduced to the power term and scaling relations were required for compression, mechanical, and motor losses. Based partly on previous assumptions, the compression loss term was limited to tip leakage (and resulting recompression of the leakage flow) and to any mismatch between built-in and system compression ratios. The effect of heat transfer on the compression process was neglected since solution of the problem is complex in the scroll compressor and was beyond the scope of the study. The shaft journals were treated as hydrodynamic and the thrust bearing as a combination of hydrodynamic and squeeze-film effects.

Coulombic friction was assumed for the flank contact zones.

Compression Loss

The same leakage model was used here as was for volumetric efficiency, except that the leakage flow represents lost compression power. The expression used for the leakage compression loss was

$$L_c = C_6 \frac{R_g(\delta + \delta_{\min})^{C_{12}}}{\sqrt{\pi R_g - R_{or} + (\delta + \delta_{\min})} C_7}$$

Shaft Bearing Loss

For a full-film hydrodynamic journal bearing in which the bearing clearance is proportional to the bearing diameter, assuming constant viscosity and L/d ratio, the viscous loss is nearly

$$L_j \propto D^3 N^2$$

Letting the compressor power be proportional to displacement and assuming a constant unit bearing load,

$$D^2 \propto R_g H$$

All journal bearings were lumped together and since the shaft speed was constant, the journal bearing loss term was

$$L_j = C_8 (R_g H)^{3/2}$$

Thrust Bearing Loss

For the full-film flat-plate bearing experiencing

an orbital motion with some tilt (wobble) under conditions of constant unit loading, the average film thickness was assumed to be proportional to the surface sliding velocity. Both the bearing area and load were proportional to Rg^2 . The bearing sliding velocity was proportional to Ror. For constant viscosity,

$$L_t \propto \frac{A_t V_t^2}{h t}$$

$$L_t = C_9 Rg^2 Ror$$

Flank Loss

Observation of flank contact zones indicate that a hydrodynamic oil film does not develop between the flanks. Analysis of flank friction power loss test results agree reasonably well with an assumption of coulombic friction. Some boundary layer or EHD lubrication may exist. The flank loss would be proportional to a friction factor, the radial inertia load less the radial gas force, and the sliding velocity.

$$L_f = f(Mos Ror \omega^2 - Fri)Ror\omega$$

The mass of the orbiting scroll was assumed to be roughly proportional to the cube of the radius of the orbiting baseplate, which scales with Rg . For constant shaft speed,

$$L_f = f Rg Ror [C_{10} Rg^2 Ror\omega - 2H(Pd-Ps)]$$

Motor Loss

Two assumptions were made regarding motor efficiency. The first was that the motor would be optimized for any given load and second that motor efficiency would increase uniformly with the motor rating.

$$\eta_m = \eta_{m0} + C_{11} W_r$$

EXPANDED EFFICIENCY EQUATION

All components of the efficiency equation were thus written using only constant coefficients and the three independent variables Ror, Rg and H . Numerical values for the constant coefficients were arrived at through a combination of calculation and empirical analysis of experimental compressors. Rather than combining all the components into a single expanded

equation to be optimized, the individual models were kept separate to make future refinements more convenient.

RESULTS

Computer Program

A computer program was written to perform the scroll dimensional optimization. A flow chart for this program is shown in Figure (7). Two of the parameters optimized, the generating radius and orbiting radius, were varied across an appropriate range in small increments. The final parameter optimized, the vane height, was related to the other parameters through the vane aspect ratio.

$$\text{Vane Aspect Ratio} = H/T$$

The vane aspect ratio was specified as a constant, since only two independent variables can be shown on a single plot. The vane aspect ratio is limited by structural constraints and practicality in the case of thin or thick vanes respectively.

For each combination of geometric parameters, the computer program calculated the mass flow, the individual loss components, and the input power. These were used to calculate the capacity and Energy Efficiency Ratio (E.E.R.). The results were stored in arrays from which lines of constant orbit radius and capacity were determined and plotted.

Discussion of Results

Figure (8) shows the results of the dimensional optimization when a typical vane aspect ratio has been specified. The plot shows that at any given capacity and vane aspect ratio there exist optimum values of the generating and orbiting radii. Also, the orbiting radius has a more significant effect on E.E.R. than the generating radius.

Figure (9) shows the overall efficiency potential as a function of capacity when all of the chosen independent variables were optimized and, in addition, the loss coefficients were minimized. This is presented as a range of possible performance bounded by two base motor efficiencies (η_{m0}). The scroll performance potential can be seen to increase with capacity and to exceed the efficiency of other compressor types now in use for air conditioning and refrigeration applications in this size range.

Refinements and Additions

Further testing and analytical calculations would allow more refined and generalized modeling of the various loss components in the scroll compressor. Areas of primary interest are 1) heat transfer, 2) bearings, 3) multiple operating conditions, 4) wider capacity range, and 5) alternate design configurations.

CONCLUSION

An overview of the analytical model derived to dimensionally optimize a scroll compressor has been presented. The objectives of the study have been met in that (1) dimensional optimization trends have been evidenced and verified experimentally and (2) efficiency potential has also been substantially predicted for various size scroll compressors.

The overall model has proven to be satisfactory although it is highly simplified and some of the individual models are not totally rigorous. However, in that regard, the authors feel that consistency between the partial and the overall idealized models is of significance, and simultaneous refinements or additions, such as those previously mentioned, are therefore to be pursued.

ACKNOWLEDGEMENT

The authors would like to acknowledge the substantial contribution to this work by Mark Bass and Roger Weatherston. The authors also wish to thank Copeland Corporation upper Management for their support and permission to publish this paper.

NOMENCLATURE

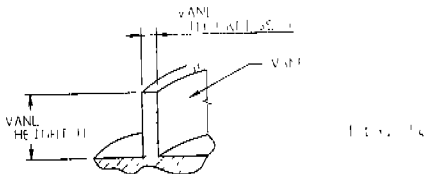
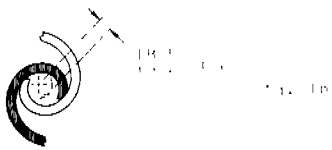
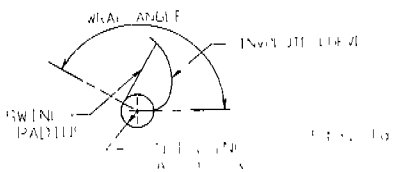
At	- Thrust Bearing Area
C ₀	- Displacement Scaling Constant
C ₁	- Tip Clearance Scaling Constant
C ₂	- Volumetric Efficiency Scaling Constant
C ₃	- Volumetric Efficiency Scaling Constant
C ₄	- Scroll Heat Transfer Scaling Constant
C ₅	- Shell Heat Transfer Scaling Constant
C ₆	- Compression Loss Scaling Constant
C ₇	- Compression Loss Scaling Constant
C ₈	- Journal Bearing Loss Scaling Constant
C ₉	- Thrust Bearing Loss Scaling Constant
C ₁₀	- Orbiting Scroll Mass Scaling Constant
C ₁₁	- Motor Efficiency Scaling Constant

C_{12} - Tip Leakage Exponent (Constant)
 C_a - Coefficient for Linear Enthalpy Approximation
 C_b - Coefficient for Linear Enthalpy Approximation
 D - Journal Bearing Diameter
 EER - Energy Efficiency Ratio (BTU/Watt-Hour)
 f - Coefficient of Sliding Friction
 F_{ri} - Radial Inertial Orbiting Scroll Force
 H - Vane Height
 H_{65} - Refrigerant Enthalpy (65°F and 90.7 psia)
 h_t - Thrust Bearing Oil Film Thickness
 L - Journal Bearing Length
 L_c - Compression Loss
 L_f - Flank Friction Loss
 L_j - Journal Bearing Loss
 L_m - Mechanical Loss
 L_t - Thrust Bearing Loss
 M_{os} - Mass of Orbiting Scroll
 \dot{m}_o - Mass Flow Rate of Oil in System
 \dot{m}_r - Mass Flow Rate of Refrigerant in System
 N - Shaft Speed (Revolutions per Unit Time)
 n - Polytropic Coefficient
 P_d - Discharge Pressure (311.5 psia at ARI A/C)
 P_d - Discharge Pressure (311.5 psia at ARI A/C)
 P_s - Suction Pressure (90.7 psia at ARI A/C)
 Q_c - Compression Heat Transferred to Vapor
 Q_e - Heat Transfer (Cooling) at Evaporator
 Q_s - Heat Transfer Through Compressor Shell
 Q_w - Waste Heat Transferred to Suction Vapor
 R_g - Involute Generating Radius
 R_o - Mass Ratio of Oil to Refrigerant in System
 R_{or} - Orbiting Radius of Scroll
 R_v - Built-in Volume Ratio of Compressor
 T - Vane Thickness
 T_s - Suction Temperature at Scroll
 V_c - Volumetric Displacement of Compressor
 (Per Revolution)
 \dot{V}_c - Volumetric Displacement Rate of Compressor
 \dot{V}_d - Volumetric Discharge Rate of Compressor
 V_t - Sliding Velocity of Thrust Bearing
 W_{in} - Electrical Input Power to Motor
 W_p - Polytropic Compression Power
 W_r - Rated Shaft Power of Motor
 Δh_e - Specific Refrigerant Enthalpy Change in
 Evaporator
 Δh_o - Specific Oil Enthalpy Change in Evaporator
 ΔH^o - Vapor Enthalpy Increase in Shell
 δ - Vane Tip Clearance
 δ_m - Minimum Initial Set-up Tip Clearance
 δ_{min} - Effective Tip Clearance Due to Composite Runout
 η - Overall Compressor Coefficient of Performance
 η_m - Motor Efficiency

- η_{mo} - Base Motor Efficiency
- η_{ph} - Preheat Efficiency (Volumetric)
- η_v - Volumetric Efficiency at Scroll Suction Conditions
- π - 3.14159265
- ρ_{65} - Density of Refrigerant Vapor (65°F and 90.7 psia)
- ω - Angular Velocity of Shaft (Radians/Second)

REFERENCES

- [1] Creux, Léon, "Rotary Engine", U.S. Pat. 801,182, 1905.
- [2] Ekelbf, J., 1933, "Rotary Pump or Compressor", U.S. Pat. 1,906,142, 1933.
- [3] Compagnie Pour La Fabrication des Compteurs et Matériel d'Usines à Gaz, "Improvements in Apparatus for Fluids Such as Engine, Pumps, Compressors, Meters and the Like, Comprising a Member Operated by an Orbital Movement", U.K. Pat. 486,192, 1938.
- [4] Sissom, L. E. and Pitts, D. R., Elements of Transport Phenomena, McGraw-Hill, 1972.



SCROLL GEOMETRIC PARAMETERS
FIGURE 1

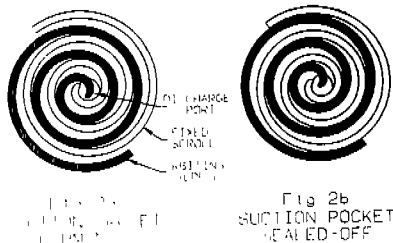


Fig 2b
SUCTION POCKET
SEALED-OFF

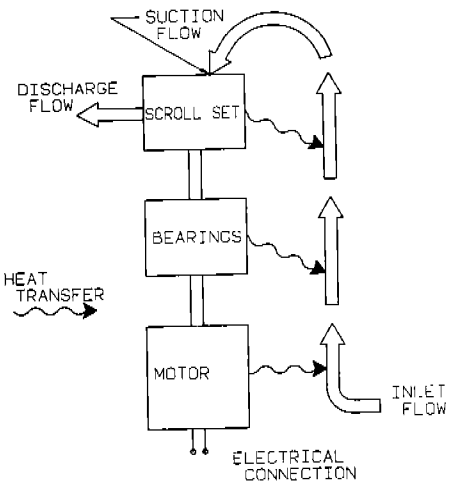


Fig 2c
DISCHARGE
INLET PISTON

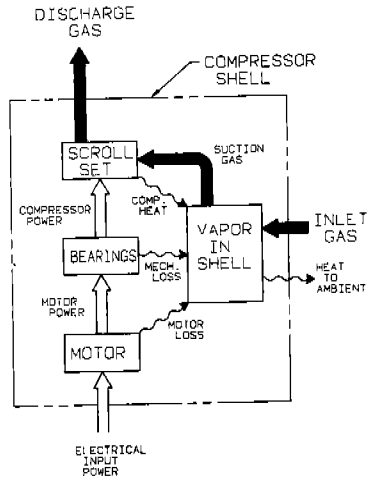


Fig 2d
POCKET
DISCHARGING

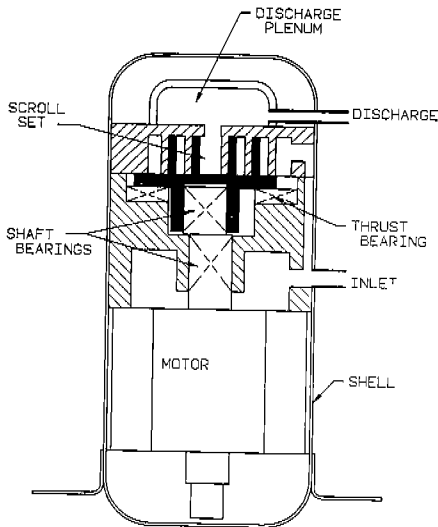
SCROLL OPERATION
FIGURE 2



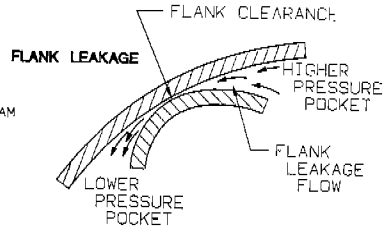
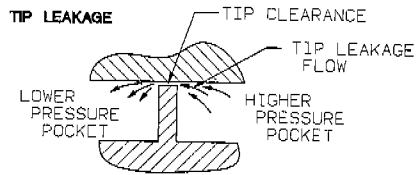
BASIC SEALED COMPRESSOR
FIGURE 3



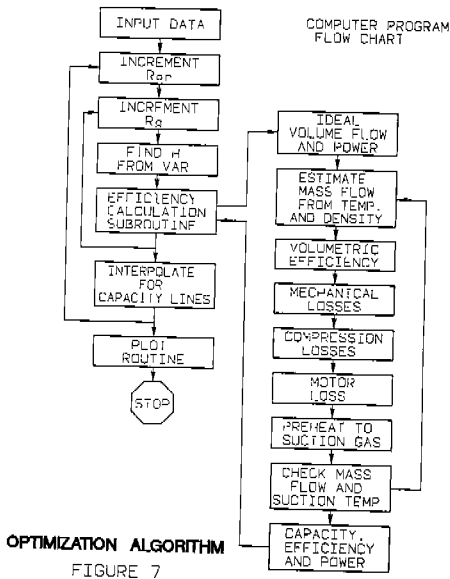
FIRST LAW MODEL
FIGURE 4



COMPRESSOR ASSEMBLY
FIGURE 5

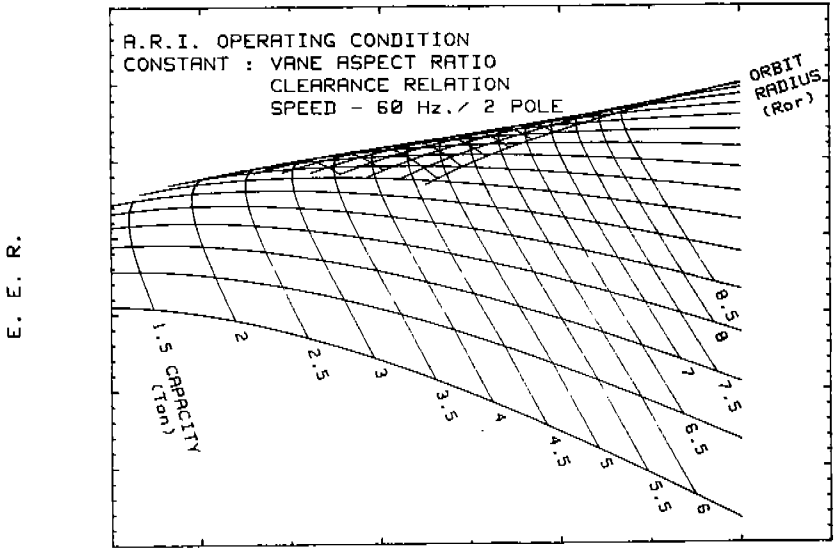


LEAKAGE FLOWS
FIGURE 6



OPTIMIZATION ALGORITHM
FIGURE 7

SCROLL DIMENSIONAL OPTIMIZATION



GENERATING RADIUS (Rg)

FIGURE 8

SCROLL EFFICIENCY POTENTIAL

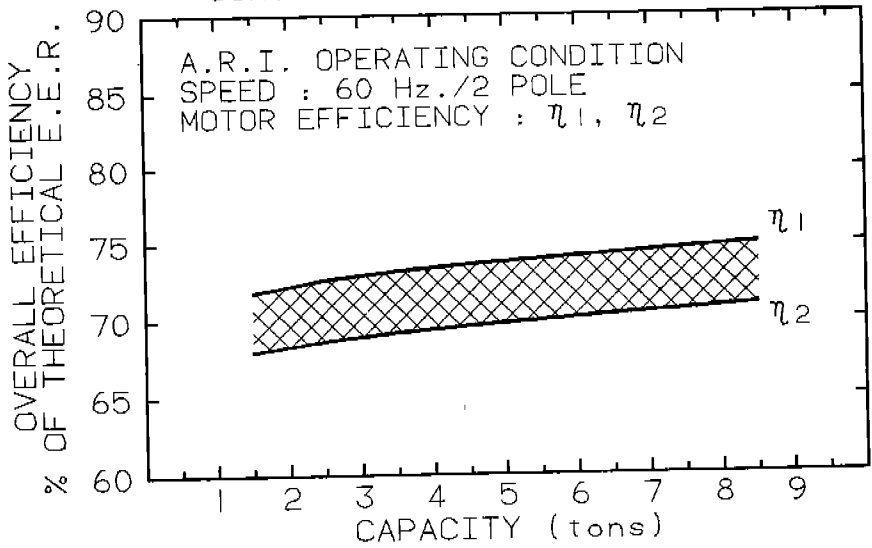


FIGURE 9